tions do not occur at room, or slightly higher, temperature under exclusion of light. The $Mo_2Cp_2(CO)_6/W_2Cp_2(CO)_6$ reaction was shown to occur photochemically, and its quantum yield was measured. In the case of the $Mn_2(CO)_{10}/Re_2(CO)_{10}$ system, which is characterized by a higher thermal stability, it has been shown that the equilibration to the heterodinuclear system $MnRe(CO)_{10}$ occurs both thermally and photochemically. Our data are complementary to those reported by Madach and Vahrenkamp.[7] From the limited amount of quantitative data available, a thermodynamic pattern appears to arise: intragroupal exchanges ($Mn_2(CO)_{10}/Re_2(CO)_{10}$, $Mo_2Cp_2(CO)_6/W_2Cp_2(CO)_6$, As_2Ph_4/P_2Ph_4) appear to be favored mainly entropically, whereas intergroupal exchanges ($Mn_2(CO)_{10}/Bi_2Ph_4$, $Cr_2Cp_2(CO)_6/E_2Ph_4$, $M_2Cp_2(CO)_6/Bi_2Ph_4$) are both entropy and enthalpy driven. Many more quantitative data should be collected before generalizations can be offered in this domain of the metal–metal single-bond-containing systems.

Acknowledgment. Financial support from the Consiglio Nazionale delle Ricerche (CNR, Roma) and from the Ministero dell'Universitā e della Ricerca Scientifica e Tecnologica (MURST) is gratefully acknowledged. We are grateful to Prof. C. A. Veracini of this department and to Dr. A. Segre, Area della Ricerca di Roma, Consiglio Nazionale delle Ricerche, for measuring the NMR spectra, to Prof. A. Morvillo, Universitā di Padova, for the mass spectra, to Prof. G. Pelizzi, Universitā di Parma, for the diffractometric experiment on $MnRe(CO)_{10}$, and to Prof. A. J. Poë, University of Toronto, for helpful discussions.

Contribution from the Department of Chemistry, University of Alberta, Edmonton, Canada T6G 2G2

Kinetics and Mechanisms of the Reaction of Oxalacetic Acid with $(H_2O)_5CrCH_2CN^{2+}$

M. J. Sisley and R. B. Jordan*

Received March 7, 1990

The reaction of $(H_2O)_5CrCH_2CN^{2+}$ with oxalacetic acid has been studied in 0.01–0.06 M H^+ at 25 °C in 1.0 M $NaClO_4/HClO_4$. The reaction was monitored at 410 and 535 nm and found to proceed in three stages assigned to complexation, chelate ring closing, and decarboxylation. The slowest stage also was studied by CO_2 collection. Complexation involves the monoanion of oxalacetate with $k_1' = 0.16\ M^{-1}\ s^{-1}$. Analysis of the complete rate law for the first two stages and of the absorbance after these stages gives estimates for monodentate dissociation ($k_{-1}' \approx 2 \times 10^{-3}\ s^{-1}$), chelate ring closing ($k_2' \approx 1 \times 10^{-4}\ s^{-1}$), chelate ring opening ($k_{-2}' \approx 2 \times 10^{-3}\ s^{-1}$), and the acid dissociation constant of the chelated hydroxy group of the enol hydrate ($K_a'' \approx 1.4 \times 10^{-2}$ M). It is suggested that decarboxylation proceeds via the protonated form of the chelated hydrate with $k_3 = 3.8 \times 10^{-2}\ s^{-1}$. The self-condensation reaction of oxalacetic acid has been characterized by ^{13}C NMR spectroscopy of the products and the variation of the yields of CO_2 with total oxalacetic acid concentration.

Introduction

Earlier studies[1,2] have shown that labile metal ions such as Mg^{2+}, Ni^{2+}, Co^{2+}, Zn^{2+}, and Cd^{2+} catalyze the decarboxylation of oxalacetic acid to pyruvate. The effectiveness of the catalysis has been correlated with the stability of the metal ion–oxalate complex, and recent work[3,4] has correlated the rates by using Marcus theory.

In dilute aqueous acid, oxalacetic acid is known[4,5] to exist in three forms, keto (I, ~13%), hydrate (II, ~80%), and enol (III,

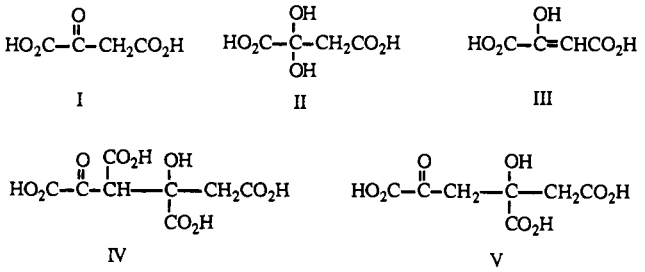

~7%), on the basis of ^1H NMR[5] spectroscopy at 38 °C and pH 1.3. In addition, it has been shown[6,7] that oxalacetic acid can undergo self-condensation to oxalocitric acid (IV), which decarboxylates to citroylformic acid (V). In the present study, self-condensation has been confirmed by ^{13}C NMR identification of the products and by measuring the reduced yield of CO_2, which results because the self-condensation product gives half as much CO_2 as that expected from oxalacetic acid decarboxylation.

The metal ion catalyst studied here ($(H_2O)_5CrCH_2CN^{2+}$) is unusual in that one aqua ligand trans to the alkyl ligand is much more labile to substitution than is typical of Cr(III) complexes; however, the four cis aqua ligands have more normal substitution lability. This aspect has been explored previously[8] with several carboxylate systems including oxalate. The consequence of this lability pattern is that it is often possible to study both first bond formation and chelate ring closing. The latter is much slower because of the relative inertness of the cis aqua ligands to be displaced. Therefore, this system presents an opportunity to observe the chelation that has been proposed[1-3] to precede decarboxylation of oxalacetic acid.

Results

The reaction of oxalacetic acid and $(H_2O)_5CrCH_2CN^{2+}$ has been observed to occur in three stages, which can be studied spectrophotometrically. The first two stages are similar in rate but show differences with observation wavelength. The third stage is due to the decarboxylation of oxalacetic acid, as confirmed by separate CO_2 collection studies. The self-condensation reaction of oxalacetic acid also has been examined briefly under our experimental conditions by using ^{13}C NMR spectroscopy to examine the products. The stoichiometry of the decarboxylation also provides evidence for the self-condensation.

Self-Condensation of Oxalacetic Acid. A solution of 0.05 M oxalacetic acid in 0.01 M perchloric acid was allowed to react for 24 h. The ^{13}C NMR spectrum revealed only peaks due to CO_2 and pyruvate species by comparison to an authentic sample of sodium pyruvate under the same conditions. The signal to noise ratio leads to the conclusion that >90% of the reaction gives pyruvate under these conditions. A similar experiment was done starting with 0.20 M oxalacetic acid, and the NMR spectrum after 24 h was much more complex and could be assigned[6,7] to a mixture of pyruvate and the hydrate of citroylformic acid. Although ^{13}C

(1) Seltzer, S.; Hamilton, G. A., Westheimer, F. H. *J. Am. Chem. Soc.* **1959**, *81*, 4018.
(2) Hay, R. W. *Rev. Pure Appl. Chem.* **1963**, *13*, 157.
(3) Leussing, D. L.; Emly, M. *J. Am. Chem. Soc.* **1984**, *106*, 443.
(4) Tsai, S.-J.; Leussing, D. L. *Inorg. Chem.* **1987**, *26*, 2620.
(5) Kokesh, F. C. *J. Org. Chem.* **1976**, *41*, 3693.
(6) Wiley, R. H.; Kim, K.-S. *J. Org. Chem.* **1973**, *38*, 3582.
(7) Buldain, G.; de los Santos, C.; Frydman, B. *Magn. Reson. Chem.* **1985**, *23*, 478.
(8) Sisley, M. J.; Jordan, R. B. *Inorg. Chem.* **1987**, *26*, 2833.

0020-1669/91/1330-1279$02.50/0

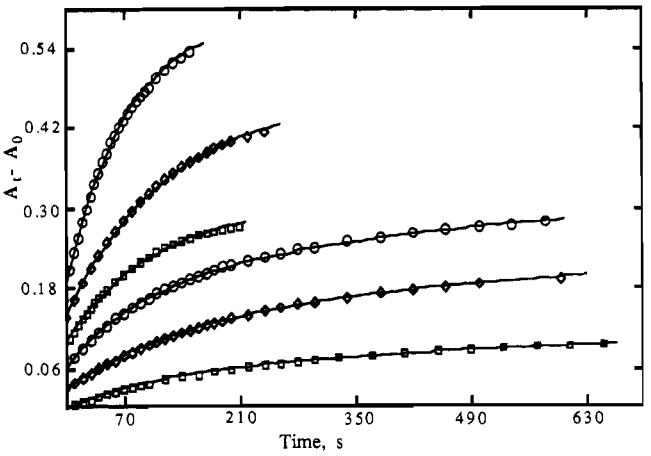

Figure 1. Time dependence of the absorbance change for the reaction of 3.8×10^{-3} M $(H_2O)_5CrCH_2CN^{2+}$ with oxalacetic acid: (○) 0.010 M H^+, 0.20 M oxalacetic acid; (◇) 0.010 M H^+, 0.10 M oxalacetic acid; (□) 0.050 M H^+, 0.20 M oxalacetic acid. For each set of conditions, the upper curve is for 410 nm and the lower curve for 535 nm. The data have been displaced vertically to improve clarity, and the curves are calculated from least-squares best fits to eq 2.

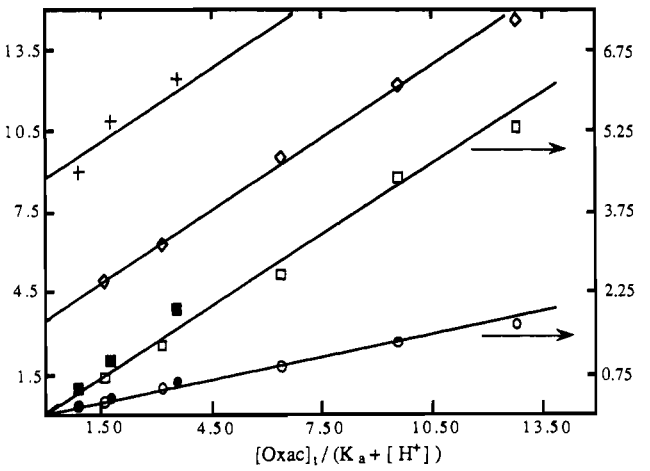

Figure 2. Results of the least-squares fits of the absorbance–time curves to eq 2: $10^3k_1(A_1 - A_0)$ at 535 nm and 0.010 M H^+ (○) and 0.050 M H^+ (●); $10^3k_1(A_1 - A_0)$ at 410 nm and 0.010 M H^+ (□) and 0.050 M H^+ (■); $10^3(\gamma_1 + \gamma_2)$ at 0.010 M H^+ (◇); $10^3(\gamma_1 + \gamma_2)$ at 0.050 M H^+ (+). The lines are from least-squares best fits to eq 5 for $k_1(A_1 - A_0)$ and to eq 7 for $(\gamma_1 + \gamma_2)$.

NMR intensities are not a reliable guide to amounts, it is clear that self-condensation is significant at the higher initial concentration of oxalacetic acid. Further studies reported below of the amount of CO_2 collected under the kinetic conditions provide more quantitative evidence for the extent of self-condensation.

First and Second Reactions of Oxalacetic Acid and $(H_2O)_5CrCH_2CN^{2+}$. Spectrophotometric observations of solutions of oxalacetic acid (0.10 M) and $(H_2O)_5CrCH_2CN^{2+}$ (9.5×10^{-4}M) in 0.011 M perchloric acid show that the absorbance increases in the 410-nm region for about 6 min and then slowly decreases. Around 535 nm, the absorbance increases for about 25 min and then slowly decreases. The absorbance increases are typical[8] of first bond formation followed by chelation and/or isomerization of a monodentate carboxylate complex.

For the absorbance increase stages, the maximum absorbances at 410 and 535 nm vary with both the $[H^+]$ and total oxalacetic acid concentration in a way consistent with a complexation reaction coming to equilibrium. However, the rate of attainment of the maximum is slower at 535 nm and shows definite biphasic character under some conditions. Some results illustrating this point are shown in Figure 1. For example, the lower three curves show that the final absorbance decreases at 535 nm when the oxalacetic acid concentration changes from 0.20 to 0.10 M in 0.010 M H^+ and the absorbance decreases further when the H^+ is raised to 0.050 M. These observations must be interpreted in terms of an equilibrium system such as the following general reaction sequence:

$$C_0 \underset{k_{-1}}{\overset{k_1}{\rightleftharpoons}} C_1 \underset{k_{-2}}{\overset{k_2}{\rightleftharpoons}} C_2 \qquad (1)$$

For such a system, the variation of the absorbance with time will be biphasic and is given by eq 2, where A_t, A_∞, and A_0 are the

$$A_t = A_\infty + \left(\frac{1}{\gamma_2 - \gamma_1}\right)\{[k_1(A_1 - A_0) - \gamma_2(A_\infty - A_0)]\exp(-\gamma_1 t) - [k_1(A_1 - A_0) - \gamma_1(A_\infty - A_0)]\exp(-\gamma_2 t)\} \qquad (2)$$

absorbances at any time, at infinite time, and at zero time, respectively, A_1 is the absorbance due to the intermediate species C_1, and k_1 is defined by eq 1. The apparent rate constants γ_1 and γ_2 are related to the rate constants in eq 1 by

$$\gamma_{1,2} = \{(k_1 + k_{-1} + k_2 + k_{-2}) \pm \sqrt{(k_1 + k_{-1} + k_2 + k_{-2})^2 - 4(k_1k_2 + k_1k_{-2} + k_{-1}k_{-2})}\}/2 \qquad (3)$$

It will be useful to note that

$$\gamma_1 + \gamma_2 = k_1 + k_{-1} + k_2 + k_{-2} \qquad (4)$$

The qualitative observation of different rates at different observation wavelengths implies that the two exponential γ terms make different contributions because of the different magnitudes of A_1, A_∞, and A_0. In order to obtain values of the γ's that are internally consistent, the absorbance–time data at both wavelengths, but the same [Oxac] and $[H^+]$, were fitted simultaneously to eq 2 to obtain values of γ_1 and γ_2, which will be wavelength independent, and $k_1(A_1 - A_0)$, which will depend on the wavelength. The main uncertainty in the analysis is the correct value of A_∞ because of the subsequent slower decarboxylation step. The values of A_∞ were determined by fitting the data to a two-exponential model (eq 2) with the smaller rate constant (γ_2) fixed at the value determined from the decarboxylation study described below. Then A_1 from these fits is taken as A_∞ for the first two stages of the reaction. These A_∞ values proved generally satisfactory, but it was noted that the magnitudes of γ_1 and γ_2 were rather sensitive to A_∞, especially when the two γ's are similar (e.g. at 0.01 M H^+ and 0.025 and 0.05 M Oxac). However the value of $\gamma_1 + \gamma_2$ is much less sensitive to A_∞ and $k_1(A_1 - A_0)$ proved to be surprisingly well defined (±5%) over a reasonable range of A_∞ values. Therefore, the subsequent analysis has concentrated on extracting kinetic information from $\gamma_1 + \gamma_2$ and $k_1(A_1 - A_0)$.

It seems reasonable to assume, on the basis of our previous work with carboxylic acids,[8] that the first step in eq 1 will be an anation reaction involving the anion of oxalacetic acid with a specific rate constant k_1' (as defined in Scheme I). If one assumes that the intermediate species (C_1) has a molar absorbancy that is independent of $[H^+]$, then the $[H^+]$ and [Oxac] dependence of $k_1(A_1 - A_0)$ should be given by eq 5. The plot[9] in Figure 2 shows that

$$k_1(A_1 - A_0) = \frac{k_1'K_a[\text{Oxac}]}{K_a + [H^+]}(A_1 - A_0) \qquad (5)$$

this expectation is satisfied by the data and gives values of $k_1'K_a(A_1 - A_0)$ of $(4.45 \pm 0.50) \times 10^{-4}$ and $(1.46 \pm 0.12) \times 10^{-4}$ at 410 and 535 nm, respectively. The same dependence is then expected for $\gamma_1 + \gamma_2$ because it also contains k_1 (see eq 4). If the second step involves addition of a second anion of oxalacetic acid, then k_2 will contribute the same type of dependence to $\gamma_1 + \gamma_2$. However, a second anation seems unlikely because we have never observed such a process with simple carboxylic acids, and when it is observed with oxalate,[8] it is preceded by observable chelation and isomerization steps. The latter processes seem to be more reasonable possibilities for the second step (C_1 to C_2) and would

(9) A value of $K_a = 5.62 \times 10^{-3}$ M has been used: Smith, R. M.; Martell, A. E. *Critical Stability Constants*; Plenum Press: New York, 1978; Vol. 3.

Scheme I

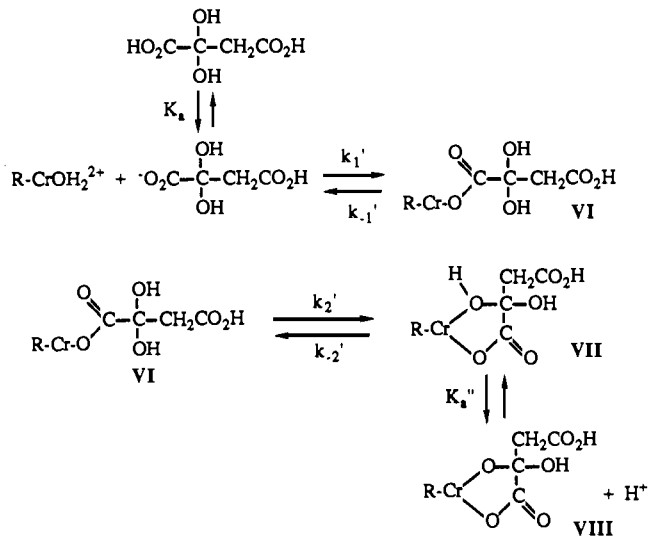

be independent of the oxalacetic acid concentration so that $\gamma_1 + \gamma_2$ might be given by eq 6. A plot of $\gamma_1 + \gamma_2$ versus $[Oxac]/(K_a + [H^+])$ is shown in Figure 2. The plot is linear, but the intercept

$$\gamma_1 + \gamma_2 = \frac{k_1'K_a[Oxac]}{K_a + [H^+]} + k_{-1} + k_2 + k_{-2} \qquad (6)$$

is larger at the higher $[H^+]$, implying that one of the last three terms in eq 6 has an $[H^+]$ dependence. We will anticipate the mechanistic interpretation by assigning the $[H^+]$ dependence to the k_{-2} term so that

$$\gamma_1 + \gamma_2 = \frac{k_1'K_a[Oxac]}{K_a + [H^+]} + k_{-1} + k_2 + k_{-2}[H^+] \qquad (7)$$

A least-squares[9] fit to eq 7 gives $k_1'K_a = (9.1 \pm 2) \times 10^{-4}$ s^{-1}, $(k_{-1} + k_2) = (2.1 \pm 1.2) \times 10^{-3}$ s^{-1}, and $k_{-2} = 0.13 \pm 0.03$ M^{-1} s^{-1}. The lines in Figure 2 represent the fit with these parameters.

A reaction sequence that is consistent with the composite rate law given by eq 7 is shown in Scheme I, where it is assumed that the dominant hydrate form is the reactant although equivalent schemes could be constructed for the keto or enol forms. According to Scheme I, the composite rate law is given by eq 8, which

$$\gamma_1 + \gamma_2 = \frac{k_1'K_a[Oxac]}{K_a + [H^+]} + k_{-1}' + k_2' + \frac{k_{-2}'[H^+]}{K_a'' + [H^+]} \qquad (8)$$

has the same form as eq 7 if $K_a'' \gg [H^+]$. Then one can calculate that $k_1' = 0.16$ M^{-1} s^{-1}, $k_{-1}' + k_2' = 2.1 \times 10^{-3}$ s^{-1}, and $k_{-2}'/K_a'' = 0.13$ M^{-1} s^{-1}. The magnitude of k_1' is consistent with values found for other carboxylate anions.[8] The results place an upper limit (including confidence limits) of $\sim 3 \times 10^{-3}$ s^{-1} on k_{-1}' and a lower limit on k_1' of ~ 0.13 M^{-1} s^{-1}, so that it is possible to estimate that $K_1 = k_1'/k_{-1}' \geq 43$ M^{-1}. This is larger than the value of 10–20 M^{-1} expected from the earlier observations on simple carboxylates, but one might invoke hydrogen-bonding interactions with the α-OH groups and coordinated H_2O to rationalize the larger K_1 value.

Although the final absorbancies (A_∞) at the end of the second stage are somewhat uncertain because of the third stage, they should be reasonably consistent with the model described in Scheme I. This model predicts that

$$A_\infty = A_0 + \{\{(A_1 - A_0)K_1[H^+] + (A_2 - A_0)K_1K_2[H^+] + (A_3 - A_0)K_1K_2K_a''\}[HOxac^-]\}/\{[H^+] + \{K_1[H^+] + K_1K_2([H^+] + K_a'')\}[HOxac^-]\} \qquad (9)$$

where A_1, A_2, and A_3 are the absorbancies due to species VI–VIII, respectively, in Scheme I. The values of $(A_1 - A_0)$ can be evaluated from the $k_1(A_1 - A_0)$ values determined above, but still there are too many parameters to be realistically evaluated from the available data. However, the results plotted in Figure 3 show that

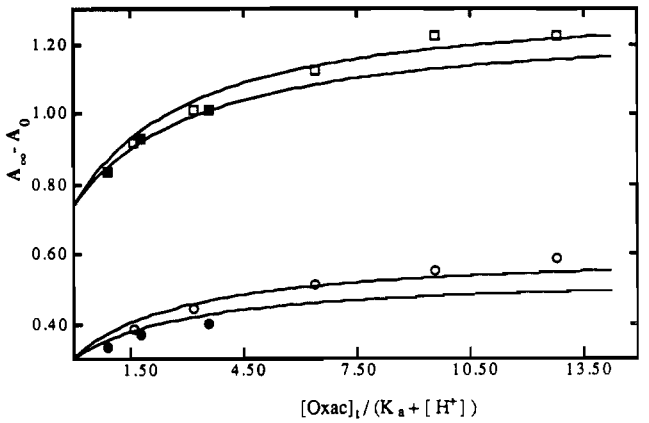

Figure 3. Variation of the maximum absorbance change $(A_\infty - A_0)$ at the end of the second stage with $[Oxac]_t/(K_a + [H^+])$. The curves are graphical fits to the equilibrium model given by eq 9 with parameters given in the text. The upper curves are for 410 nm with 0.01 M H^+ (□) and 0.05 M H^+ (■); the lower curves are at 535 nm with 0.10 M H^+ (○) and 0.05 M H^+ (●).

the A_∞ values at least are consistent with reasonable parameters for the model. The curves in Figure 3 are for $K_1 = 50$, $K_1K_2 = 3.3$, $K_1K_2K_a'' = 0.045$, $(A_2 - A_0) = 0.89$ and 0.88 at 410 and 535 nm, respectively, and $(A_3 - A_0) = 1.61$ and 1.33 at 410 and 535 nm, respectively. These can be used to estimate that $K_a'' \approx 1.4 \times 10^{-2}$ M, $k_{-2}' \approx 1.8 \times 10^{-3}$ s^{-1}, and $k_2' \approx 1 \times 10^{-4}$ s^{-1}, which is not inconsistent with the value of $k_{-1}' + k_2' = 2.1 \times 10^{-3}$ s^{-1}.

Chromium(III) Products after the Second Stage. Product identification in this system is inevitably difficult and of indirect relevance to the primary process because of the multiple stages and the fact that coordinated oxalacetate will continue to decarboxylate during the product separation procedure. Nevertheless, we have briefly examined the products essentially after the second stage. A solution containing 0.10 M oxalacetic acid and 9.0×10^{-3} M $(H_2O)_5CrCH_2CN^{2+}$ in 0.01 M $HClO_4$ was allowed to react for 10 min and then treated with $Hg(ClO_4)_2$ to remove the $-CH_2CN$ group. This also precipitated mercury(II) oxalacetate, which was redissolved by adding NaCl before the solution was diluted to an ionic strength of ~0.1 M and loaded onto a column of Dowex 50W-X8 (Na^+). About 30% of the total chromium(III) passed through the column to yield a very dilute solution with absorbance maxima at 415 and 549 nm and extinction coefficients of ~69 and 55 M^{-1} cm^{-1}, respectively. Another 30% of the chromium was eluted from the column under conditions typical of a 2+ ion. The remaining 40% is $Cr(OH_2)_6^{3+}$ and $(H_2O)CrNCCH_2Hg^{4+}$, which derive[10] from uncomplexed $(H_2O)_5CrCH_2CN^{2+}$. The first fraction could be the deprotonated pyruvate chelate analogous to VIII, and the next could be a mixture of pyruvate species analogous to VI and VII. The 40% of uncomplexed chromium(III) is reasonably consistent with the 32% that can be calculated from the equilibrium constants for Scheme I as discussed in the preceding section. Kinetic results for the first and second stages are summarized in Table I.

CO_2 Evolution and the Third Spectrophotometric Stage. The third stage observed spectrophotometrically has the same apparent rate as that for CO_2 evolution, measured manometrically. Therefore, the third stage is assigned to decarboxylation.

The absorbance versus time and CO_2 pressure versus time curves are reasonably represented by a first-order rate law with a pseudo-first-order rate constant that is essentially independent of the oxalacetic acid concentration, increases with increasing $[(H_2O)_5CrCH_2CN^{2+}]$, and decreases with increasing $[H^+]$. The kinetic observations from the spectrophotometric and CO_2 collection methods are summarized in Table II. The simplicity of the kinetic behavior comes as a relief but also as a surprise because the logical extension of Scheme I would predict that the decarboxylation step should be described by Scheme II. If the complexation reactions in Scheme I are treated as rapidly established

(10) Sisley, M. J.; Jordan, R. B. *Inorg. Chem.* **1986**, *25*, 3547.

Table I. Kinetic Results from the Data at 410 and 535 nm for the First and Second Stages of the Complexation of $(H_2O)_5CrCH_2CN^{2+}$ by Oxalacetic acid (25 °C, 1.0 M $NaClO_4/HClO_4$)

$10^2[H^+]$, M	$10[OxAc]_{tot}$, M	$10^3[CrCH_2CN]$, M	$10^3k_1(A_1 - A_0)$,[a,c] s^{-1}	$10^3(\gamma_1 + \gamma_2)$,[c] s^{-1}
1.00	0.251	3.80	0.670	4.90
1.00	0.499	3.80	1.26	6.24
1.00	1.00	3.80	2.57	9.48
1.00	1.50	3.80	4.35	12.2
1.00	2.00	3.80	5.28	14.6
5.00	0.500	2.94	0.535[b]	8.96
5.00	0.500	3.80	0.975	10.8
5.00	2.0	3.80	1.92	12.4

[a] These are values at 410 nm and those at 535 nm average 3.1 times smaller. [b] This value has been corrected by 3.8/2.94 for the difference in Cr(III) concentration to make it comparable to the other values. [c] These values are determined from least-squares fits of the data at both wavelengths to eq 2; from various fits with different A_∞ values, the range is ±5% for $k_1(A_1 - A_0)$ and ±15% for $(\gamma_1 + \gamma_2)$.

Scheme II

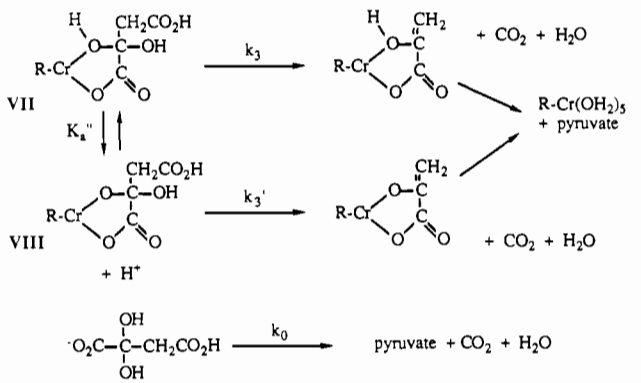

equilibria relative to the decarboxylation, then the rate of production of CO_2 is given by eq 10, where the constants a and b

$$\frac{d[CO_2]}{dt} = \left[\left\{\frac{(k_3K_1K_2[H^+] + k_3'K_1K_2K_a'')K_a[Cr\text{-}R]}{[H^+](K_a + [H^+])}\Big/\left(1 + \frac{K_a(K_1[H^+] + K_1K_2[H^+] + K_1K_2K_a'')[Oxac]}{[H^+](K_a + [H^+])}\right)\right\} + k_0\right][Oxac] = \left[\left\{\frac{a}{1 + b[Oxac]}\right\} + k_0\right][Oxac] \quad (10)$$

are defined by a term by term comparison and k_0 is the rate constant for the uncatalyzed reaction. The second term in the denominator involving [Oxac] indicates a more complex than first-order behavior could be expected for the decarboxylation. The integrated rate law[11] contains a first-order term with a rate constant $(a + k_0)$ and a second-order term that contains b. The results from the previous section allow us to estimate b, and numerical analysis shows that the second-order term makes a small contribution so that only $(a + k_0)$ can be evaluated realistically. The values of $(a + k_0)$ are only about 5–7% larger than the apparent rate constant from a simple first-order rate law and are satisfactorily described by eq 11. Observed and calculated values

$$a + k_0 = \frac{((7.02 \pm 1.3) \times 10^{-4})[Cr\text{-}R]}{K_a + [H^+]} + \frac{((2.31 \pm 1.3) \times 10^{-5})[H^+] + (5.43 \pm 3.5) \times 10^{-7}}{K_a + [H^+]} \quad (11)$$

(11) The integrated rate law is given by

$$t = \left(\frac{1}{a + k_0}\right) \ln\left\{\frac{[Oxac]_0 - [CO_2]_0}{[Oxac]_0 - [CO_2]}\right\} + \left(\frac{a}{a + k_0}\right) \ln\left\{\frac{a + k_0 + k_0b([Oxac]_0 - [CO_2]_0)}{a + k_0 + k_0b([Oxac]_0 - [CO_2])}\right\}$$

Table II. Rate Constants for the Third Spectrophotometric Stage and for the Decarboxylation by CO_2 Collection[a] (25 °C, 1.0 M $NaClO_4/HClO_4$)

$[H^+]_0$, M	$[H^+]_{av}$,[b] M	$[OxAc]_{tot}$, M	$10^3[CrCH_2CN]$, M	$10^4(a + k_0)$, s^{-1}	
				obsd[a]	calcd[c] (a)[d]
0.010	0.010	0.10	1.05	0.86	1.04 (0.55)
0.010	0.0105	0.050	2.10	1.31	1.40 (0.93)
0.010	0.0112	0.100	2.10	1.33	1.35 (0.89)
0.010	0.0128	0.200	2.10	1.33	1.26 (0.81)
0.020	0.0235	0.100	2.10	0.84	0.88 (0.51)
0.050	0.058	0.100	2.10	0.45	0.53 (0.23)
0.010	0.011	0.100	5.24	2.52	2.67 (2.25)
0.010	0.0197	0.150	0.0	0.404	0.394 (0.0)
0.010	0.0119	0.100	1.12	0.97	0.92 (0.46)
0.010	0.0105	0.050	2.24	1.76	1.46 (0.99)
0.010	0.0111	0.100	2.24	1.51	1.42 (0.96)
0.010	0.0119	0.150	2.24	1.44	1.37 (0.91)
0.010	0.0126	0.200	2.24	1.36	1.32 (0.88)
0.020	0.0233	0.100	2.24	1.05	0.92 (0.55)
0.020	0.0249	0.200	2.24	0.94	0.81 (0.46)
0.050	0.053	0.100	2.24	0.52	0.54 (0.25)
0.050	0.059	0.200	2.24	0.57	0.49 (0.21)
0.010	0.0106	0.100	4.75	2.47	2.54 (2.09)
0.010	0.0104	0.100	7.25	3.73	3.67 (3.23)
0.010	0.011	0.200	7.25	3.43	3.54 (3.12)

[a] The first seven entries are from spectrophotometric observations at 410 nm, and the remainder are from CO_2 collection. The spectrophotometric results have 95% confidence limits ≤5%, and the CO_2 collection limits are larger at ≤10% because of the fewer data points. [b] Calculated average $[H^+]$ taking into account the difference in acidity of oxalacetic acid and the product pyruvate. [c] Calculated from a least-squares fit to eq 12. [d] Calculated values of 10^4a, the contribution of the $Cr\text{–}CH_2CN^{2+}$ catalyzed path.

Table III. Calculated and Observed Yields of CO_2 from the Decarboxylation of Oxalacetic Acid

$10^2[H^+]_{av}$, M	$10[Oxac]_t$, M	$10^3[Cr\text{–}R]$, M	% yield of CO_2	
			obsd	calcd[a]
1.05	0.50	2.24	99.5	94.4
1.11	1.00	2.24	90.5	90.2
1.19	1.50	2.24	83.4	86.3
1.26	2.00	2.24	82.2	83.2
1.19	1.00	1.12	84.5	86.4
1.00	1.11	2.24	90.4	89.7
1.06	1.00	4.75	100	93.7
1.04	1.00	7.25	97.0	95.4
2.33	1.00	2.24	89.0	86.3
2.49	2.00	2.24	78.0	78.9
5.30	1.00	2.24	81.4	81.4
5.90	2.00	2.24	72.7	73.3

[a] Calculated with $k_{2D} = 3.78 \times 10^{-4}$ s^{-1} as determined from a least-squares fit to eq 13.

are compared in Table II. Comparison to the theoretical expression for a (eq 10) reveals that the k_3' term is not making a significant contribution and that $k_3K_1K_2K_a = 7.0 \times 10^{-4}$. The value[9] of K_a and our previous estimate of $K_1K_2 \approx 3.3$ allow one to calculate that $k_3 \approx 3.8 \times 10^{-2}$ s^{-1}. The expression for k_0 is consistent with uncatalyzed decarboxylation of oxalacetic acid with a rate contant of 2.3×10^{-5} s^{-1} and of its conjugate base with

Scheme III

$$A \xrightarrow{k_{1C}} B + CO_2$$

$$2A \longrightarrow A_2 \xrightarrow{k_{2D}} C + CO_2$$

a rate constant of $5.4 \times 10^{-7}/K_a = 1 \times 10^{-4}$ s^{-1}. The latter values are not well determined because k_0 is generally a small contribution to $(a + k_0)$, but the relative values are consistent with earlier work,[12] which indicates that the conjugate base is the more reactive species.

The CO_2 collection technique also allows us to determine the moles of CO_2 produced per mole of oxalacetic acid and thereby assess the extent of formation and decarboxylation of oxalocitric acid (IV). The yields of CO_2 under various conditions are summarized in Table III. Qualitatively these yields decrease with increasing concentration of oxalacetic acid as expected because the dimerization is a second-order process, and they increase with increasing $(H_2O)_5CrCH_2CN^{2+}$ because the catalytic process tends to remove oxalacetic acid in competition with the dimerization. A quantitative assessment can be given in terms of the reactions in Scheme III, where A is oxalacetic acid, A_2 is oxalocitric acid, B is pyruvate, and C is citroylformate. The apparent rate constants k_{1C} and k_{2D} may contain contributions from the spontaneous and the catalyzed decarboxylation reactions of A and A_2. If a steady state is assumed for A_2, then the ratio of total CO_2 produced to the initial oxalacetic acid (A_0) is given by eq 12, where $c = k_{1C}/k_{2D}$. The data were analyzed by assuming that k_{1C} is given

$$\frac{[CO_2]_f}{[A_0]} = 0.50 + \frac{c}{4[A_0]} \ln\left(1 + \frac{2[A_0]}{c}\right) \qquad (12)$$

by eq 11, and a least-squares fit gives $k_{2D} = 3.8 \pm 0.7 \times 10^{-4}$ s^{-1}. The observed and calculated values are compared in Table III. Since oxalocitric acid is largely in the protonated form under our conditions, k_{2D} represents the rate constant for decarboxylation of the acid.

Summary and Conclusions

The study of the reaction of $(H_2O)_5CrCH_2CN^{2+}$ with oxalacetic acid has shown that the sequence of reactions is complexation, followed by ring closure, and then decarboxylation. This sequence has been inferred from studies on much more labile metal ions.[2,4] A comparison of the rate constants derived from eq 12 shows that oxalacetate coordinated to $(H_2O)_5CrCH_2CN^{2+}$ decarboxylates at least 10^2–10^3 more rapidly than the free anion or acid, respectively.

The analysis of the equilibrium data (eq 9) gives an estimate for the acidity of the coordinated –OH group $K_a'' \approx 1.4 \times 10^{-2}$ M. This value is consistent with that of 8.3×10^{-2} M[13] for the equivalent ionization of the pyruvate chelate of $(H_2O)_4Cr^{3+}$, since charge effects would predict that the latter should be more acidic than $(NCCH_2)(H_2O)_3Cr^{2+}$. Water molecules coordinated to Cr(III) are expected to have pK_a values in the 3–4 range, so that the coordinated –OH is apparently about 100 times more acidic than coordinated H_2O.

Several details of the mechanism remain uncertain. For example, the chelate ring closing step to form VII in Scheme I might proceed by attack of coordinated water on the α-carbon of the monodentate oxalacetate. There is precedent for this[14] in the chelate ring closing of the oxalato complex *cis*-$[Co(en)_2(C_2O_4H)(OH_2)]^{2+}$. The rate constant for ring closing in the $NCCH_2$–Cr^{2+} system ($<2 \times 10^{-3}$ s^{-1}) is smaller than that for oxalate (2.75×10^{-2} s^{-1}),[8] but this is to be expected given the different types of entering functions involved.

Scheme IV

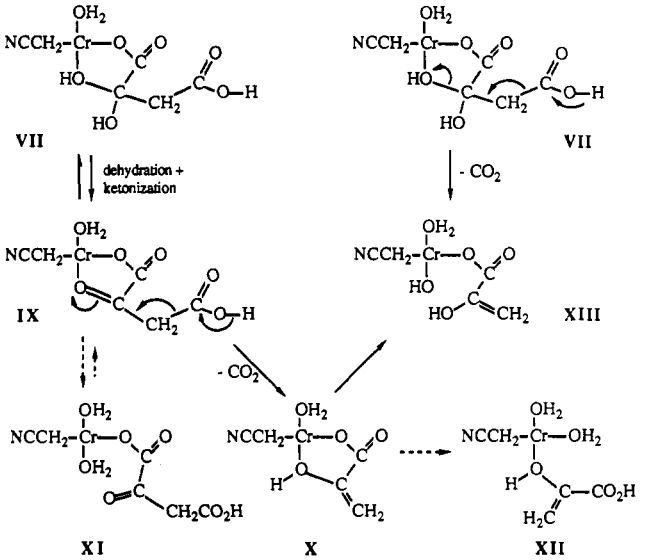

The details of the decarboxylation step (k_3 in Scheme II) are uncertain. Two possibilities are shown in Scheme IV. The traditional mechanism[2-4] for metal ion catalysis proceeds through the keto form (IX),[15] which decarboxylates to X followed by ring opening to XIII. The latter will lose pyruvate from the labile position trans to the alkyl group to regenerate the catalyst. This mechanism is based on studies with labile metal ions, generally in the region of pH 6, where the dominant species (~87%) is the keto form of the dianion[5] and where the enolate complex is found to be inactive. Our observations agree that the enolate complex (VIII in Scheme I) is inactive. However, our acidity conditions are such that the enol complex (VII) is a major species and decarboxylation might proceed directly from this species to XIII, as shown in Scheme IV. The mechanism involving the keto form has several potential problems for the $(H_2O)_5CrCH_2CN^{2+}$ system. The decarboxylation of IX must be competitive with ring opening to XI. Available evidence[16,17] indicates that a ketonic oxygen, at least in acetone and methylacetate, is very weakly coordinating and ring opening of IX would be expected to be a facile process. It also seems probable that X would ring open to XII in preference to XIII, because the position trans to the alkyl group is much more labile. This should cause a reduction and eventual loss of catalytic activity. The direct reaction of VII to XIII avoids these complications and does not violate the previous conclusions that the enolate complex is inactive.

Experimental Section

The $(H_2O)_5CrCH_2CN^{2+}$ solutions were prepared by the reaction of aqueous Cr(II) and ICH_2CN followed by ion-exchange separation of the product.[18] Cr(II) was prepared by dissolving chromium metal in perchloric or trifluoromethane sulfonic acid rather than by zinc amalgam reduction of Cr(III) in order to ensure that the solutions were free of Zn(II), which catalyzes the decarboxylation of oxalacetic acid. The preparation of other standard reagents has been described previously.[8,19] Oxalacetic acid (Sigma Chemical Co.) was used as supplied after being characterized by C:H analysis and ^{1}H NMR spectroscopy.

Spectrophotometric kinetic observations were initiated by mixing a fresh solution of oxalacetic acid with a solution of $(H_2O)_5CrCH_2CN^{2+}$, with each solution containing appropriate amounts of $HClO_4$ and $NaClO_4$ to give the desired final acidity and ionic strength. When the oxalacetic acid would contribute more than the desired amount of H^+, these solutions were partially neutralized with standard NaOH. The reaction was monitored on a Cary 219 spectrophotometer equipped with

(12) Gelles, E. *J. Chem. Soc.* **1956**, 4736.
(13) Sisley, M. J.; Jordan, R. B. *Inorg. Chem.* **1989**, *28*, 2714.
(14) Miskelly, G. M.; Clark, C. R.; Buckingham, D. A. *J. Am. Chem. Soc.* **1986**, *108*, 5202.
(15) A reviewer has suggested that step VII to IX could be rate controlling in our system.
(16) Hurst, J. K.; Taube, H. *J. Am. Chem. Soc.* **1968**, *90*, 1174.
(17) Dixon, N. E.; Jackson, W. G.; Lancaster, M. L.; Lawrance, G. A.; Sargeson, A. M. *Inorg. Chem.* **1981**, *20*, 470.
(18) Kupferschmidt, W. C.; Jordan R. B. *J. Am. Chem. Soc.* **1984**, *106*, 991.
(19) Sisley, M. J.; Jordan, R. B. *Inorg. Chem.* **1987**, *26*, 273.

a standard temperature-controlled (±0.2 °C) water flow system. Observations at 410 and 535 nm were done on independent kinetic runs. Trial experiments on a stopped-flow system, mixing fresh solutions of oxalacetic acid with acidic solutions of $(H_2O)_5CrCH_2CN^{2+}$, indicate that there are no fast absorbance changes preceding those that could be observed on the Cary 219 instrument.

The CO_2 collection studies were done in all glass apparatus connected to a mercury manometer to monitor the CO_2 evolution. A freshly prepared solution of oxalacetic acid was temperature equilibrated for ~5 min in the reaction vessel, and then a similarly equilibrated solution of $(H_2O)_5CrCH_2CN^{2+}$ was injected from a syringe through a stopcock. The apparatus was evacuated with a water aspirator and then closed, and pressure measurements were started about 1 min after mixing. The reaction vessel was immersed in a water bath on a temperature-regulated (±1 °C) hot plate. The overall pressure change depended on the amount of oxalacetic acid and was typically in the range 80-150 mmHg. The volume of the gas collection system was calibrated by weighing the amount of water required to fill the apparatus.

The ^1H and ^{13}C NMR spectra were recorded on a Bruker AM 300 spectrometer. The ^{13}C chemical shifts were measured relative to 5% dioxane, which has a shift of 67.4 ppm relative to TMS. The ^{13}C chemical shifts (relative to TMS) for various functional groups fall into well-defined regions that are rather independent of the chemical species as follows: CH_3(keto), 26 ppm; CH_3(hydrate), 27 ppm; $C(OH)_2$, 93.6 ppm; CO_2H(keto), 168 ppm; CO_2H(hydrate), 174-178 ppm; CO(keto), 202 ppm; dissolved CO_2 was observed at 124.45 ppm.

Acknowledgment. We acknowledge the financial support of the Natural Sciences and Engineering Research Council of Canada.

Contribution from the Department of Chemistry, University of Minnesota, Minneapolis, Minnesota 55455, and Science Research Laboratory, 3M Central Research Laboratories, St. Paul, Minnesota 55144

Electrochemistry and Infrared Spectroelectrochemistry of $[(\eta^5\text{-}C_5R_5)Fe(CO)_2]_2$ (R = H, Me): Generation and Characterization of $[(\eta^5\text{-}C_5R_5)Fe(CO)_2]_2(PF_6)$ Complexes

John P. Bullock,[†] Michael C. Palazotto,[‡] and Kent R. Mann*,[†]

Received September 6, 1990

The electrochemistry of $[CpFe(CO)_2]_2$ (Cp = η^5-cyclopentadienyl) was reexamined under a variety of conditions. This compound, and the related species $[Cp^*Fe(CO)_2]_2$ (Cp^* = η^5-pentamethylcyclopentadienyl), exhibit irreverisble net two-electron oxidations in CH_3CN/TBAH ($E_{p,a}$ = 0.68 and 0.33 V vs AgCl/Ag, respectively) but undergo two, one-electron oxidations in CH_2Cl_2/TBAH. For $[CpFe(CO)_2]_2$, these occur at 0.68 and 1.28 V, while in the $[Cp^*Fe(CO)_2]_2$ complex they occur at 0.34 and 1.16 V. The first process is quasi-reversible for each compound and generates the corresponding binuclear radical cations. The binuclear radical cations were generated and characterized via UV-vis and infrared spectroelectrochemistry. $[CpFe(CO)_2]_2^+$ exists as a mixture of the cis and trans carbonyl-bridged isomers in solution with ν(CO) at 2023, 2055, and 1934 cm^{-1}. $[Cp^*Fe(CO)_2]_2^+$ exists only as the trans isomer in solution with λ_{max} = 518 nm and ν(CO) at 1987 and 1884 cm^{-1}. The binuclear radical-cation species $[CpFe(CO)_2]_2^+$ has long been invoked as an intermediate in the oxidation chemistry of $[CpFe(CO)_2]_2$ but has never been cleanly generated or characterized prior to this work. EPR spectra were observed for both radical cations. $[CpFe(CO)_2]_2^+$ has $g_\parallel$ = 2.004 and $g_\perp$ = 2.084, while $[Cp^*Fe(CO)_2]_2^+$ has $g_\parallel$ = 1.999 and $g_\perp$ = 2.088. These cations are susceptible to rapid, ligand-induced disproportionation reactions. When the ligand is acetonitrile, the proposed mechanisms of these reactions involve the generation and subsequent decomposition of acetonitrile adducts of the radical cation species, e.g., $\{[CpFe(CO)_2]_2(NCCH_3)\}^+$. For the Cp^* compound, the intermediate is short-lived. Stopped-flow measurements of the reaction of $[Cp^*Fe(CO)_2]_2^+$ with CH_3CN showed that the reaction is first order in $[[Cp^*Fe(CO)_2]_2^+]$ and $[CH_3CN]$ with k = 118 (±2) M^{-1} s^{-1}. Cyclic voltammetry studies detected the Cp-containing intermediate $\{CpFe(CO)_2]_2(NCCH_3)\}^+$. The initially formed decomposition products, in the case of $[CpFe(CO)_2]_2^+$, are the 18-electron cationic species $[CpFe(CO)_2(NCCH_3)]^+$ and the 17-electron radical $CpFe(CO)_2^\cdot$. In subsequent reactions, the latter species generates $[CpFe(CO)_2]_2$ and, to a lesser extent, $CpFe(CO)_2Cl$.

Introduction

The electrochemistry of metal-metal bonds has been an area of active research for several years.[1,2] Among the most frequently studied compounds in this area has been $[CpFe(CO)_2]_2$.[2-7] In 1966, Dessy and co-workers reported that the formal iron-iron bond can be reductively cleaved via a net two-electron process at mercury electrodes.[2] Miholová and Vlcek later studied the reduction process in detail and reported that it occurs via an ECE mechanism involving an initial diffusion-controlled electron transfer.[3] The electrochemical oxidation of $[CpFe(CO)_2]_2$ has also been studied. In 1971, Meyer and co-workers published a report that discussed the electrooxidation of $[CpFe(CO)_2]_2$ in a variety of solvents.[4] It was found that in coordinating solvents, e.g., acetonitrile, the oxidation proceeds by two electrons and yields the monomeric metal-solvent adduct cation (eq 1). In

$$[CpFe(CO)_2]_2 \xrightarrow{CH_3CN} 2[CpFe(CO)_2(NCCH_3)]^+ + 2e^- \quad (1)$$

CH_2Cl_2/TBAH, while the overall oxidation was also reported to proceed by two electrons, it was proposed to proceed via an initially generated one-electron oxidized species; no direct observation of this intermediate was reported however. Later, the electrochemistry of this compound was reexamined, also in CH_2Cl_2/TBAH, and was found to exhibit a reversible one-electron oxidation (E° = +0.67 V vs SCE), followed by a second, irreversible oxidation peak at 1.21 V.[7] An attempted bulk electrolysis of the dimer between the two oxidation processes, however, resulted in the removal of two electrons per dimer and generation of a species assigned as $CpFe(CO)_2(PF_6)$.

* To whom correspondence should be addressed.
[†] University of Minnesota.
[‡] 3M Central Research Laboratories.

(1) For leading articles in this field, see: (a) Dessy, R. E.; Stary, F. E.; King, R. B.; Waldrop, M. *J. Am. Chem. Soc.* **1966**, *88*, 471. (b) Dessy, R. E.; Weissman, P. M.; Pohl, R. L. *J. Am. Chem. Soc.* **1966**, *88*, 5117. (c) Denisovich, L. I.; Ioganson, A. A.; Gubin, S. P.; Kolobova, N. E.; Anisimov, K. N. *Bull. Acad. Sci. USSR, Div. Chem. Sci. (Engl. Transl.)* **1969**, *18*, 218. (d) Pickett, C. J.; Pletcher, D. *J. Chem. Soc., Dalton Trans.* **1975**, 879. (e) Meyer, T. J. *Prog. Inorg. Chem.* **1975**, *19*, 1. (f) Lemoine, P.; Giraudeau, A.; Gross, M. *Electrochim. Acta* **1976**, *21*, 1. (g) Lemoine, P.; Gross, M. *J. Organomet. Chem.* **1977**, *133*, 193. (h) de Montauzon, D.; Poilblanc, R.; Lemoine, P.; Gross, M. *Electrochim. Acta* **1978**, *23*, 1247. (i) Madach, T.; Vahrenkamp, H. *Z. Naturforsch., B: Anorg. Chem., Org. Chem.* **1979**, *34B*, 573. (j) Connelly, N. G.; Geiger, W. E. *Adv. Organomet. Chem.* **1984**, *23*, 1. (k) Lacombe, D. A.; Anderson, J. E.; Kadish, K. M. *Inorg. Chem.* **1986**, *25*, 2074. (l) Jaitner, P.; Winder, W. *Inorg. Chim. Acta* **1987**, *128*, L17.
(2) Dessy, R. E.; Weissman, P. M.; Pohl, R. L. *J. Am. Chem. Soc.* **1966**, *88*, 5117.
(3) Miholová, D.; Vlcek, A. A. *Inorg. Chim. Acta* **1980**, *41*, 119.
(4) Ferguson, J. A.; Meyer, T. J. *Inorg. Chem.* **1971**, *10*, 1025.
(5) Moran, M.; Cuadrado, I.; Losada, J. *Inorg. Chim. Acta* **1986**, *118*, 25.
(6) Davies, S. G.; Simpson, S. J.; Parker, V. D. *J. Chem. Soc., Chem. Commun.* **1984**, 352.
(7) Legzdins, P.; Wassink, B. *Organometallics* **1984**, *3*, 1811.

0020-1669/91/1330-1284$02.50/0